Pharm Res (2015) 32:2912–2927
DOI 10.1007/s11095-015-1673-7

RESEARCH PAPER

Modulation of Pharmacokinetic and Cytotoxicity Profile of Imatinib Base by Employing Optimized Nanostructured Lipid Carriers

Biki Gupta • Bijay Kumar Poudel • Tuan Hiep Tran • Roshan Pradhan • Hyuk-Jun Cho • Jee-Heon Jeong • Beom Soo Shin • Han-Gon Choi • Chul Soon Yong • Jong Oh Kim

Received: 20 December 2014 / Accepted: 9 March 2015 / Published online: 5 May 2015

ABSTRACT

Purpose To prepare, optimize and characterize imatinib-loaded nanostructured lipid carriers (IMT-NLC), and evaluate their pharmacokinetic and cytotoxicity characteristics.

Methods IMT-NLC was prepared by hot homogenization method, and optimized by an approach involving Plackett-Burman design (PBD) and central composite design (CCD). An *in vivo* pharmacokinetic study was conducted in rats after both oral and intravenous administration. The *in vitro* cytotoxicity was evaluated by MTT assay on NCI-H727 cell-lines.

Results PBD screening, followed by optimization by CCD and desirability function, yielded an optimized condition of 0.054, 6% *w/w*, 2.5% *w/w* and 1.25% *w/v* for organic-to-aqueous phase ratio (O/A), drug-to-lipid ratio (D/L), amount of lecithin (Lec) and amount of Tween® 20 (Tw20) respectively. The optimized IMT-NLC exhibited a particle size (S_z) of 148.80 ± 1.37 nm, polydispersity index (PDI) 0.191 ± 0.017 of and ζ-potential of −23.0 ± 1.5 mV, with a drug loading (DL) of 5.48 ± 0.01% and encapsulation efficiency (EE) of 97.93 ± 0.03%. IMT-NLC displayed sustained IMT release *in vitro*, significantly enhanced *in vivo* bioavailability of IMT after intravenous and oral administration, and greater *in vitro* cytotoxicity on NCI-H727 cells, compared with free IMT.

Conclusion A combined DoE approach enabled accurate optimization and successful preparation of IMT-NLC with enhanced *in vivo* pharmacokinetic and *in vitro* cytotoxicity characteristics.

KEY WORDS nanostructured lipid carrier · imatinib base · Plackett-Burman design · central composite design · bioavailability

ABBREVIATIONS

ANOVA	Analysis of variance
ATP	Adenosine triphosphate
CCD	Central composite design
CML	Chronic myeloid leukemia
DoE	Design of Experiments
DL	Drug loading
D/L	Drug-to-total lipid ratio
DLS	Dynamic light scattering
DSC	Differential scanning calorimetry
DST	Dasatinib
EE	Encapsulation efficiency
FDA	Food and Drug Administration
HPLC	High performance liquid chromatography
IMT	Imatinib
IV	Intravenous
LbM	Labrafil M 1944 CS
LcN	Lecithin
Lec	Amount of lecithin
NLC	Nanostructured lipid carrier
O/A	Organic-to-aqueous phase ratio

Electronic supplementary material The online version of this article (doi:10.1007/s11095-015-1673-7) contains supplementary material, which is available to authorized users.

B. Gupta • B. K. Poudel • T. H. Tran • R. Pradhan • H.-J. Cho • J.-H. Jeong • C. S. Yong (✉) • J. O. Kim (✉)
College of Pharmacy Yeungnam University, 214-1, Dae-Dong Gyeongsan 712-749 South Korea
e-mail: csyong@yu.ac.kr
e-mail: jongohkim@yu.ac.kr

B. S. Shin
College of Pharmacy Catholic University of Daegu, Gyeongsan 712-702 South Korea

H.-G. Choi (✉)
College of Pharmacy, Institute of Pharmaceutical Science and Technology Hanyang University, 55, Hanyangdaehak-ro Sangnok-gu Ansan 426-791 South Korea
e-mail: hangon@hanyang.ac.kr

PBD	Plackett-Burman design
PBS	Phosphate-buffered saline
PcA	Precirol ATO 5
PDGFR	Platelet-derived growth factor receptor
PDI	Polydispersity index
QbD	Quality by Design
SD	Standard deviation
SLN	Solid lipid nanoparticles
TEM	Transmission electron microscopy
TwN	Tween® 20
Tw20	Amount of Tween® 20
UV	Ultraviolet
XRD	X-ray diffraction

INTRODUCTION

Nanostructured lipid carriers (NLCs), new generation of solid lipid nanoparticles (SLNs), are lipid-based nanocarriers with a hybrid lipid core composed of a mixture of a solid lipid and a spatially incompatible liquid lipid. NLCs combine the advantages associated with SLNs (ease of encapsulation of hydrophobic as well as hydrophilic drug, ability to impart sustained release characteristics upon incorporated drug, ability to shield the drug from chemical, photochemical or oxidative degradation, ability to immobilize the drug in a solid matrix, ease of scale-up and manufacture, low cost, and extremely low toxicity) with the capability to incorporate large quantities of drugs, and overcome the drawback of drug expulsion from the lipid core [1, 2].

Recently, a number of researchers have reported the potential of using NLC to deliver anticancer drugs as individual agents or in combination, as well as genetic materials *via* oral, intravenous (IV), pulmonary, and intraperitoneal routes of administration [3–9]. NLCs offer critical advantages, including improved solubility and enhanced bioavailability of poorly soluble drugs, protection of encapsulated drugs from degradation by pH and enzymes, protection of the body from drug toxicity, enhanced storage stability, modulation of drug release, increased specificity and tumor targeting, and capability to attain large-scale production output. Immense potential, therefore, exists for their application in cancer chemotherapy [10, 11].

Imatinib (IMT) is a potent and specific inhibitor of protein tyrosine kinase Bcr-Abl, platelet-derived growth factor receptors PDGFRα and PDGFRβ, and c-Kit receptors. It exerts cytotoxicity activity by binding to the ATP-binding segment of the kinase domain, thereby preventing subsequent phosphorylation of downstream proteins. It is practically insoluble in water (0.001 g/ 100 ml), rendering it highly impracticable for administration [12]. The mesylate salt of IMT is marketed by Novartis under the trade name Gleevec®, which has been approved for Philadelphia chromosome positive chronic myeloid leukemia (CML), PDGFR gene rearrangement-associated myelodysplastic/myeloproliferative diseases, hypereosinophilic syndrome, chronic eosinophilic leukemia, dermatofibrosarcoma protuberans, and malignant gastrointestinal stromal tumors [13].

With the growing realization that simply increasing product testing does not improve product quality, the Food and Drug Administration (FDA) has recently increased emphasis upon Quality by Design (QbD). Control strategy is an important aspect of QbD, which includes defining design spaces around individual or multiple unit operations amongst others. A design space is the multidimensional combination and interaction of input variables and process parameters that have been demonstrated to provide assurance of quality, which can be determined by employing suitable Design of Experiments (DoE) approach [14]. DoE helps to construct a useful predictive model of all critical responses and facilitates identification of all potential variables and their simultaneous systematic and rapid evaluation. It helps to optimize the levels of all significant variables and allows the researchers to obtain an optimum combination of excipients and processes within the total multidimensional experimental region [15]. A DoE approach, involving an initial screening by Plackett-Burman design and fractional factorial design, followed by optimization with a response surface design such as central composite design and Box-Behnken design, is prescribed specially for processes where a large number of variables are involved [16].

In our present study, we prepared a novel NLC loaded with IMT (base), an anti-cancer drug with poor aqueous solubility. The NLC system was optimized using a combination of two DoE approaches, *i.e.*, PBD and CCD. Thereafter, we characterized the optimized formulation and evaluated the *in vitro* release characteristics, *in vivo* pharmacokinetic profile, and *in vitro* cytotoxicity.

MATERIALS AND METHODS

Materials

IMT and dasatinib (DST) were obtained from LC Laboratories (Woburn, Massachusetts, USA). Precirol® ATO 5 (PcA, glyceryl distearate) and Labrafil® M 1944 CS (LbM, oleoyl polyoxy-6 glycerides) were obtained from Gattefosse (St Priest, France). Tween® 20 (TwN, polysorbate 20) and lecithin (LcN) were purchased from Samchun Chemicals (Seoul, Korea) and Junsei (Tokyo, Japan) respectively. Deionized water was prepared as per requirement using Milli Q-water purification system (Millipore, MA, USA). Other chemicals were reagent-grade, and were used without further purification.

Method of HPLC Analysis for Imatinib

Quantification of IMT was performed by a modification of a reported HPLC method [17]. HPLC system (Hitachi, Tokyo, Japan) comprised L-2130 pump, L-2200 autosampler, L-2420 UV–vis detector and L-2350 column oven with Ezchrom elite software (version 318a). An Inertsil C_8 column (250 mm × 4.6 mm, 5 μm particle size; GL Sciences Inc., Tokyo, Japan) was used under isocratic elution of 0.02 M monobasic potassium phosphate/acetonitrile (6:4, v/v) mobile phase at a flow rate of 1.0 ml/min and column temperature of 25.0 ± 1.0°C. For each analysis, 20 ml aliquot of the sample was injected and the UV absorbance was measured at a wavelength of 265 nm. The calibration plots exhibited exceptional linearity (R^2 = 0.999) over 0.1–100 μg/ml concentration range and the RSD of the plot over different periods of time was below 3%.

Selection of Lipids

Since the encapsulation of a drug in a lipid core depends to a great extent on its lipid solubility, we tested the capacity of a number of liquid lipids to solubilize IMT [18]. An excess of IMT was added to 1 ml of each liquid lipid in a 2-ml microtube (Axygen MCT-200) and mixed by vortexing for 1 min. The samples were shaken for 72 h in a water-bath shaker at 100 strokes per min and 25°C, and subsequently centrifuged at 5000 × *g* for 10 min. The supernatants were filtered through a 0.45-μm membrane filter and diluted using the mobile phase for subsequent analysis by HPLC.

Four solid lipids (Compritol 888 ATO, CmA; Precirol ATO 5, PcA; Gelucire 44/14, GlC; and Sappocire AP, SpA) were tested by preparing sixteen blank NLC formulations at predefined level of variables (Table S1) using all combinations with the liquid lipids selected on the basis of the above solubility studies. The lipid combinations exhibiting acceptable DLS (Dynamic Light Scattering) characteristics (S_z, PDI) were used to prepare IMT-loaded NLC formulations, with D/L of 0.05, for final selection of the most appropriate solid lipid/liquid lipid pair.

Preparation of NLC formulations

IMT-NLC was prepared by "hot homogenization method" involving homogenization and sonication. The solid lipid (PcA) was dissolved at 70°C and mixed with the liquid lipid (LbM) to constitute the organic phase used to dissolve LcN. IMT was subsequently added and dissolved by stirring at 50 rpm for 10 min. For the aqueous phase, TwN was dissolved in purified water and heated to 70°C. The aqueous phase was added to the organic phase using a 10 ml disposable syringe and homogenized using high-performance homogenizer (ULTRA-TURRAX® T25, IKA). The resulting primary emulsion was sonicated using a probe sonicator (Vibra-Cell™, SONICS) and cooled in an ice bath for 3 h to obtain IMT-NLC. Blank NLC (b-NLC) was prepared using the same procedure, omitting the addition of IMT. The scheme of IMT-NLC system has been presented in Fig. 1.

Design of Experiments

Plackett-Burman design

An 11-factor PBD at 2 levels was utilized for initial screening of the main effects of 8 variables (Table I) on the characteristics of IMT-NLC. The lower and upper levels of the 8 variables were selected on the basis of prior preliminary experiments. A total of 15 experimental runs, including 3 center point replicates, were generated by virtue of Design-Expert® 8.0.7.1 software (Stat-Ease Inc., Minneapolis, MN, USA) and carried out in a random fashion. The effects of the tested variables were studied on 3 responses: DL (y_1), EE (y_2) and S_z (y_3). Variables not significant for the assessed responses were identified and omitted from further optimization.

Central Composite Design

A 4-factor CCD was employed for final optimization of main effects, interaction effects and quadratic effects of the formulation variables on *in vitro* performance of the IMT-NLC. In CCD, each numeric factor is varied over 5 levels: 2 axial points (+α and -α), two factorial points (+1 and −1) and the center point. The 5 levels of the 4 studied variables have been shown in Table I. The default value of "α" for a 4-factor

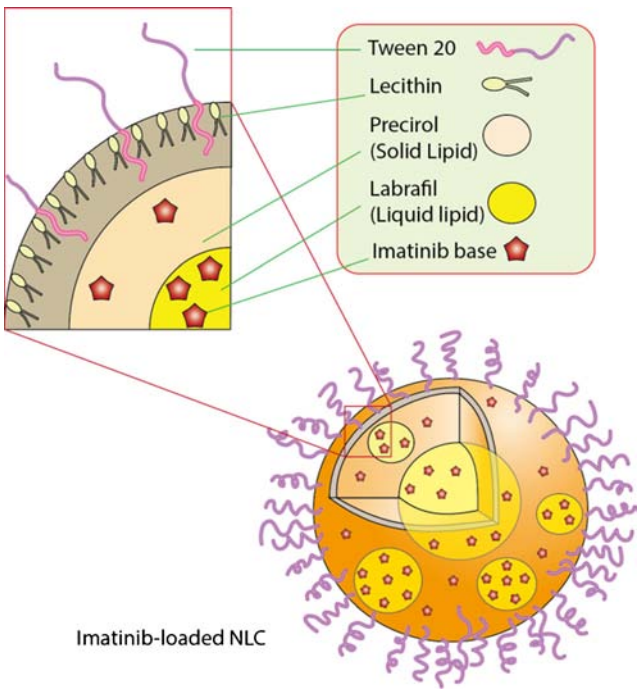

Fig. 1 Scheme of imatinib-loaded nanostructured lipid carrier system.

Table I Variables for Plackett-Burman design and central composite design

Plackett-Burman design					
Variables		Lower level		Upper level	
x_1: Oil to total lipid ratio, O/L		0.30		0.50	
x_2: Organic to aqueous phase ratio, O/A		0.02		0.06	
x_3: Amount of Lecithin, Lec[a]		2% w/w		6% w/w	
x_4: Amount of Tween 20, Tw20[b]		1% w/v		3% w/v	
x_5: Drug to total lipid ratio, D/L		0.04		0.06	
x_6: Homogenization time, HT		9 min		15 min	
x_7: Sonication time, ST		6 min		10 min	
x_8: Sonication amplitude, SA		60%		80%	
Central composite design					
Variables	Central point	Factorial points		Axial points	
		−1	+1	−α	+α
X_1: O/A	0.04	0.025	0.055	0.01	0.07
X_2: D/L	0.05	0.04	0.06	0.03	0.07
X_3: Lec[a]	4%w/w	2.5%w/w	5.5%w/w	1%w/w	7%w/w
X_4: Tw20[b]	2%w/v	1.25%w/v	2.75%w/v	0.5%w/v	3.5%w/v

Three dummy variables (x_9: dummy1, x_{10}: dummy2, and x_{11}: dummy3) also were employed in Plackett-Burman design.

[a] relative to total lipid

[b] relative to aqueous phase

rotatable design is 2, while the recommended number of center point replicates, so that the design gives a good estimate of experimental error and an accurate test for lack of fit, is 6. A total of 30 experimental runs were generated using Design-Expert® software. The response factors studied for assessing the *in vitro* performance of IMT-NLC were DL (Y_1), EE (Y_2), cumulative *in vitro* drug release over 36 h (Rel_{36}, Y_3) and S_z (Y_4). The results for each of the response factors were fitted to a quadratic polynomial model described by the following nonlinear equation.

$$Y = \beta_0 + \beta_1 X_1 + \beta_2 X_2 + \beta_3 X_3 + \beta_4 X_4 + \beta_5 X_1 X_2 + \beta_6 X_1 X_3 + \beta_7 X_1 X_4 + \beta_8 X_2 X_3 + \beta_9 X_2 X_4 + \beta_{10} X_3 X_4 + \beta_{11} X_1^2 + \beta_{12} X_2^2 + \beta_{13} X_3^2 + \beta_{14} X_4^2 + \varepsilon$$

Where Y is the individual response factor or dependent variable; β_0-β_{14} are regression coefficients; ε is the error; and X_1, X_2, X_3 and X_4 are the independent variables.

Optimization Using Desirability Functions

Desirability functions approach for optimization of multiple responses, introduced by Derringer and Suich [19], was used to optimize all 4 responses following the generation of model polynomials that establish the relationship between dependent and independent variables using Design-Expert® software. The four responses: Y_1, Y_2, Y_3, and Y_4 were transformed into individual desirability values d_1, d_2, d_3, and d_4 respectively, and goals for each response were defined. A number of solutions were generated by Design-Expert software, which was arranged in the decreasing order of their global desirability value. The solution having the highest desirability value is considered to be the most optimal solution, and hence is used for preparation of the optimized formulation.

Characterization of IMT-NLC

Particle Size, Polydispersity and ζ-Potential

The hydrodynamic particle size, PDI, and ζ-potential IMT-NLC were investigated by DLS method using a Nano-S90 ZetaSizer (Malvern Instruments, Worcestershire, UK). The measurements were conducted at a fixed scattering angle of 90° and at an equilibrated temperature of 25°C. Samples were adequately diluted with distilled water prior to measurement, and 3 measurements were performed for each sample.

Drug Loading and Encapsulation Efficiency

DL and EE were determined by ultracentrifugation. A 2 ml aliquot of IMT-NLC was taken into an Amicon® Ultra-4 10 K centrifugal filter device (molecular wright cut-off 10 kDa; Merck Millipore Ltd., Ireland), centrifuged at 4500 rpm for 10 min, and the concentration of the free drug

in the filtrate was measured by HPLC. DL and EE were calculated by using the following formulae:

$$DL(\%) = \left\{(W_T - W_u)\Big/(W_L + W_T - W_U)\right\} \times 100$$

$$E\ E\ (\%) = \left\{(W_T - W_U)\Big/W_T\right\} \times 100$$

Here, W_T, W_U and W_L denote weight of total drug initially added, weight of unbound drug, and weight of total lipid, respectively.

Transmission Electron Microscopy

Transmission electron microscopy (TEM) was used to demonstrate the size and morphology of IMT-NLC. A drop of IMT-NLC was deposited onto a copper grid coated with a carbon film, and the particles were subjected to negative staining by phosphotungstic acid (2%, *w/v*). The sample was then dried under mild to moderate infrared radiation and observed under an H7600 transmission electron microscope (Hitachi, Tokyo, Japan).

Solid-State Characterization of IMT-NLC

Lyophilization of the Formulation

IMT-NLC, along with a blank NLC formulation, was pre-frozen at −70°C for 12 h and subsequently lyophilized (freeze-dried) at −40°C for 24 h using EYELA® Freeze Dryer (Tokyo Rikakikai Co. Ltd., Tokyo, Japan). Upon completion of freeze drying, the samples were allowed to dry at 20°C for an additional 12 h.

Differential Scanning Calorimetry

Freeze-dried IMT-NLC and blank NLC were used for solid state characterization by differential scanning calorimetry (DSC). A DSC-Q200 differential scanning calorimeter (TA Instruments, New Castle, DE, USA) was used to observe thermal characteristics of IMT-NLC, blank NLC, and IMT. The DSC scans were accomplished by heating all the samples from 20 to 250°C at a heating rate of 20°C /min in a dynamic nitrogen atmosphere.

X-ray Diffraction

A vertical goniometer and X-ray diffractometer (X'pert PRO MPD diffractometer, Almelo, The Netherlands) was used to observe the X-ray diffraction (XRD) patterns of freeze-dried IMT-NLC against freeze-dried blank NLC, and IMT. The diffractometer measured Ni-filtered CuKα-radiation (voltage, 40 kV; current, 30 mA) scattered in the crystalline regions of the sample. The XRD scans were performed over a diffraction angle (2θ) range of 10°–60° and a scanning rate of 5°/min.

Physical Stability Study

Physical stability of IMT-NLC was investigated upon storage at of 4°C over 60 days. Aliquots were taken following 1, 3, 7, 15, 30, and 60 days of storage and S_z, PDI, and EE were evaluated as described above.

In Vitro Release Study

In vitro release was evaluated by dialysis method. Briefly, IMT-NLC (1 ml, equivalent to 3 mg of IMT) or free IMT (3 mg/ml in Labrafil M 1944 CS) was taken in a dialysis bag (molecular weight cut-off 3.5 kD), which had been hydrated overnight beforehand in phosphate-buffered saline (PBS) pH 7.4. The dialysis bag was clipped on both sides and then kept in USP Type II dissolution apparatus containing 400 ml of PBS pH 7.4 (with 1% v/v TwN), maintained at a temperature of 37 ± 0.5°C. The paddles were operated at 50 rpm, and 2 ml of the medium was withdrawn at defined time intervals, replacing each time with same amount of fresh medium. Drug concentrations in the samples were determined by HPLC.

Pharmacokinetic Evaluation

Administration and Blood Collection

Twenty adult male Sprague–Dawley (SD) rats were divided randomly into two groups (group 1 & group 2) of 10 rats each. Both groups were further sub-divided into two sub-groups of 5 rats each. All the animals were housed at 20 ± 2°C and relative humidity of 50–60%, and were fasted for 12 h prior to drug administration. All animal-handling procedures were in accordance with the protocols approved by the Institutional Animal Ethical Committee, Yeungnam University, South Korea.

Rats belonging to group 1 were administered free IMT (sub-group 1) or IMT-NLC (sub-group 2) by IV injection into the left femoral vein at a dose of 10 mg/kg body weight. Free IMT (0.5% w/v) for IV administration was prepared by dissolving IMT in PEG 400 (20% v/v in water for injection). Rats belonging to group 2 were administered free IMT (sub-group 1) or IMT-NLC (sub-group 2) by oral route at a dose of 20 mg/kg body weight. Free IMT (0.5% w/v) for oral administration was prepared by dispersing IMT in 0.5% w/v polyvinyl pyrrolidone K 30 solution. Higher dose was administered by oral route with due regards to relatively lower bioavailability associated with oral route of administration. Blood samples (approximately 300 μl each) were withdrawn from right femoral arteries of the animals 0.25, 0.5, 1, 2, 4, 6, 9,

12, 18 & 24 h post-injection for group 1, and 0.5, 1, 2, 4, 6, 9, 12, 18 & 24 h following oral administration for group 2. Samples were collected in 2 ml-microtubes containing heparin solution (80 IU/ml) and immediately centrifuged at 10, 000 rpm for 10 min. After centrifugation, plasma (100 µl) was withdrawn and stored in a 2 ml-microtube at −20°C.

Plasma Sample Analysis

To each 2 ml-microtube containing plasma (100 µl), internal standard (10 µl of 0.05% w/v DST) and acetonitrile (100 µl, as extracting solvent) were added. The samples were mixed by vortexing for 30 min and centrifuged at 10,000 rpm for 10 min. The supernatant was analyzed using a modification of the HPLC approach described above, with 0.025% v/v formic acid/acetonitrile (7.5:2.5, v/v) used as the mobile phase at a flow rate of 1.0 ml/min. 20-µl aliquots were injected into the column and UV detection was performed at 265 nm. The calibration plots exhibited exceptional linearity ($R^2 = 0.998$) over 0.1–100 µg/ml concentration range and the RSD of the plot over different periods of time was below 3%.

Pharmacokinetic Data Analysis

Pharmacokinetic profiles of free IMT and IMT-NLC following IV and oral administration were determined using WinNonlin™ software (standard edition, version 2.1; Pharsight Corporation, Mountain View, CA, USA). Non-compartmental analyses were performed to quantify area under the plasma concentration–time curve from time zero to infinity ($AUC_{0-\infty}$), plasma half-life ($T_{1/2}$), elimination rate constant (K_e), plasma clearance (Cl), and mean residence time (MRT). Peak plasma concentration (C_{max}) and time to reach C_{max} (T_{max}) were calculated for oral administration.

Cytotoxicity Assay

3-(4,5-Dimethylthiazol-2-yl)-2,5-diphenyltetrazolium bromide (MTT) assay was used to evaluate *in vitro* cytotoxicity of free IMT, blank NLC, and IMT-NLC in human bronchial carcinoid cell-line NCI-H727. Briefly, cells (1 x 10^4) were seeded into flat-bottomed 96-well plates and allowed to adhere at 37°C for 24 h in 10% fetal bovine serum-supplemented RPMI 1640 medium. The medium was removed from each well and dilutions of IMT, IMT-NLC and blank NLC (in serum-free RPMI medium) were added. After 48-h incubation at 37°C, the medium was removed, the wells were washed twice with PBS, and MTT (100 µl, 1.25 mg/mL) was added. Following incubation for 3 h at 37°C in the dark, the cells were lysed, and the formazan crystals were dissolved by adding 100 µL DMSO to each well. The number of viable cells was determined by measuring the absorbance at 570 nm using a microplate reader (Multiskan EX, Thermo Scientific, Waltham, MA, USA). Cell viability was calculated using the formula: cell viability = $A_{sample} / A_{control} \times 100\%$, where A stands for absorbance at 570 nm.

RESULTS

Selection of Lipids

Selection of liquid lipid was based upon the saturation solubility of IMT in the liquid lipid. Saturation solubility values of IMT in various liquid lipids/oils have been presented in Table II. Labrafac lipophile WL 1349 (LfW), Labrafil M 1944 CS (LbM), Labrafil M 2125 CS (LbF), and Labrafil WL 2609 BS (LbW) exhibited considerably higher solubilizing capacity for IMT. These were used to combine with four solid lipids (CmA, PcA, GlC, SpA) to prepare sixteen NLC formulations (Table S2). Eight formulations (BF-1, BF-4, BF-5, BF-8, BF-9, BF-12, BF-13, and BF-16) degraded physically soon after preparation, where the particles appeared to accumulate and settled at the bottom of the container, and thereby, were considered inappropriate. DLS characteristics of the remaining eight are shown in Table S2. Acceptable DLS characteristics included $S_z < 200$ nm and PDI < 0.200. Formulations BF-2, BF-3, BF-6, and BF-7, which satisfied the specified criteria, were used to prepare IMT-NLC formulations, with D/L of 0.05 (Table S3). The pair of PcA and LbM (corresponding to F-3) exhibited the smallest S_z with the highest EE,

Table II Saturation solubility of imatinib in various oils

Liquid lipids / Oils	Saturation solubility at 25°C (µg/mL)[a]
Capryol 90	11.52 ± 3.14
Capryol PGMC	17.19 ± 0.44
Castor oil	76.97 ± 15.92
Cottonseed oil	42.16 ± 14.49
Labrafac lipophile WL 1349	1649.99 ± 146.87
Labrafac PG	173.10 ± 8.48
Labrafil M 1944 CS	2304.89 ± 212.77
Labrafil M 2125 CS	2449.34 ± 412.73
Labrafil WL 2609 BS	1649.99 ± 146.87
Labrasol	448.42 ± 5.84
Lauroglycol FCC	40.39 ± 1.28
Peanut oil	21.85 ± 3.41
Sesame oil	25.30 ± 7.00
Sorbitan sesquioleate	116.93 ± 5.77
Sunflower oil	17.58 ± 2.63

[a] each value represented as mean ± SD ($n = 3$)

and was therefore selected for preparation of IMT-NLC and optimization by DoE.

Plackett-Burman Design

PBD matrix and the observed responses are shown in Table S4. The effects of different variables on DL, EE, and S_z are shown in Fig. 2. D/L and O/A exhibited significant effects on DL ($P<0.01$; Fig. 2a), O/A ($P<0.01$), D/L, Lec, and Tw20 ($P<0.05$) significantly affected EE (Fig. 2b). O/A and Tw20 exhibited significant effects on S_z ($P<0.05$; Fig. 2c). Based on these observations, O/A, D/L, Lec, and Tw20 were selected for further optimization by CCD.

Central Composite Design

Statistical Analysis

The observed response values are summarized alongside each run in the CCD matrix presented in Table S5. Each response was individually fitted to a second-order quadratic model, and statistical parameters comprising ANOVA, lack-of-fit tests, and multiple correlation coefficient (R^2) tests were used to determine model significance. Results of statistical evaluations are illustrated in Table III. Correlation coefficients are presented in Table S6.

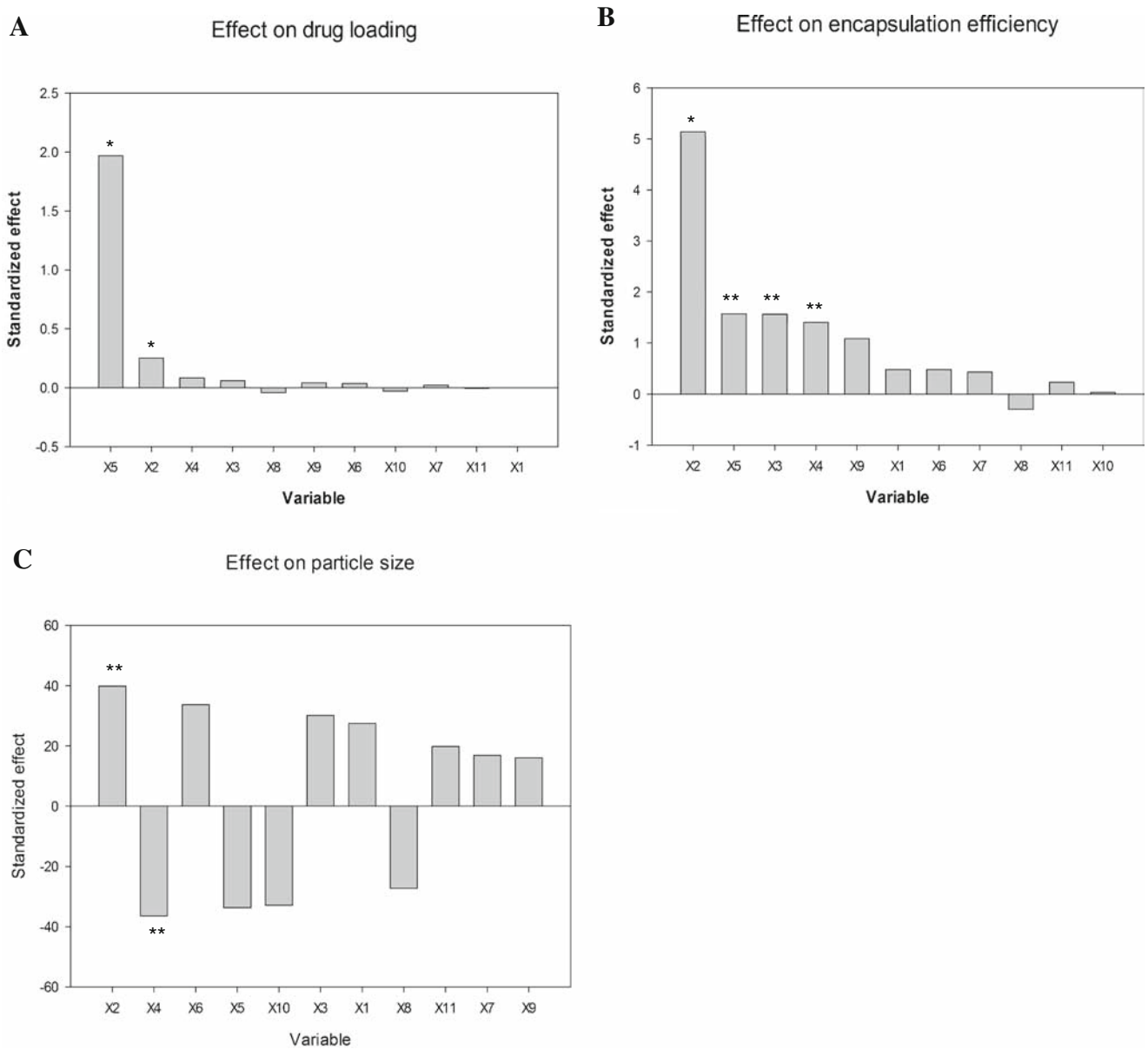

Fig. 2 Plackett–Burman design (PBD): effects on drug loading (**a**), encapsulation efficiency (**b**), and particle size (**c**). X1: oil-to-total lipid ratio (O/L); X2: organic-to-aqueous phase ratio (O/A); X3: amount of lecithin (Lec); X4: amount of Tween® 20 (Tw20); X5: drug-to-total lipid ratio (D/L); X6: homogenization time (HT); X7: sonication time (ST); X8: sonication amplitude (SA); X9: dummy1; X10: dummy2; X11: dummy3. *significant at $P<0.01$; **significant at $P<0.05$.

Table III ANOVA for the Response Surface Reduced Models

	Source	Sum of Squares	df	Mean Square	*F*-value	*p*-value
Quadratic Model						
Y_1: Drug Loading	Model	20.64	4	5.16	6291.39	<0.0001
	X_1-O/A	*0.12*	*1*	*0.12*	*152.22*	*<0.0001*
	X_2-D/L	*20.41*	*1*	*20.41*	*24884.38*	*<0.0001*
	X_3-Lec	*0.068*	*1*	*0.068*	*83.11*	*< 0.0001*
	X_1^2	*0.038*	*1*	*0.038*	*45.86*	*< 0.0001*
	Residual	0.021	25	8.203×10^{-4}		
	Lack of Fit	*0.019*	*20*	9.440×10^{-4}	*2.90*	*0.1203* [a]
	Pure Error	1.626×10^{-3}	*5*	3.252×10^{-4}		
	Cor Total	20.66	29			
Y_2: Encapsulation Efficiency	Model	93.98	3	31.33	78.35	< 0.0001
	X_1-O/A	*61.60*	*1*	*61.60*	*154.06*	*< 0.0001*
	X_2-D/L	*14.45*	*1*	*14.45*	*36.13*	*< 0.0001*
	X_1^2	*17.94*	*1*	*17.94*	*44.87*	*< 0.0001*
	Residual	10.40	26	0.40		
	Lack of Fit	*9.63*	*21*	*0.46*	*3.00*	*0.1127* [a]
	Pure Error	*0.76*	*5*	*0.15*		
	Cor Total	104.38	29			
Y_4: Particle Size	Model	36953.37	5	7390.67	311.26	< 0.0001
	X_1-O/A	*8877.44*	*1*	*8877.44*	*373.87*	*< 0.0001*
	X_4-Tw20	*12221.69*	*1*	*12221.69*	*514.71*	*< 0.0001*
	X_1X_4	*7969.28*	*1*	*7969.28*	*335.63*	*< 0.0001*
	X_1^2	*2304.48*	*1*	*2304.48*	*97.05*	*< 0.0001*
	X_4^2	*6332.01*	*1*	*6332.01*	*266.67*	*< 0.0001*
	Residual	569.87	24	23.74		
	Lack of Fit	*526.42*	*19*	*27.71*	*3.19*	*0.1014* [a]
	Pure Error	*43.45*	*5*	*8.69*		
	Cor Total	37523.24	29			
Linear Model						
Y_3: Drug Release at 36 h	Model	1782.19	2	891.10	18.12	< 0.0001
	X_1-O/A	*573.21*	*1*	*573.21*	*11.66*	*0.0020*
	X_4-Tw20	*1208.98*	*1*	*1208.98*	*24.59*	*< 0.0001*
	Residual	1327.58	27	49.17		
	Lack of Fit	*1220.02*	*22*	*55.46*	*2.58*	*0.1483* [a]
	Pure Error	*107.56*	*5*	*21.51*		
	Cor Total	3109.77	29			

The insignificant factors were excluded from the model to obtain a better fit

[a] no significant difference at $P < 0.1$

At 5% significance level, models corresponding to responses Y_1, Y_2, and Y_4 exhibited the best fit to quadratic model, while model corresponding to response Y_3 showed the best fit to linear model (Table S7). Lack-of-fit for each model was determined to be insignificant ($P > 0.1$; Table III), indicating that the models exhibited a good fit to the responses. Individual model terms found to be significant ($P < 0.05$) are presented in Table III. Factor terms X_1^2 and X_4^2 indicate quadratic effects, while X_1X_4 indicates an interaction effect. The factor terms corresponding to other interaction effects (X_1X_2, X_1X_3, X_2X_3, X_2X_4, and X_3X_4) and those indicating other quadratic effects (X_2^2, X_3^2) were found to be insignificant, and were therefore excluded from the model. Exclusion of insignificant model terms in the construction of the model ensures a better fit.

O/A (X_1), D/L (X_2), and Lec (X_3) exhibited significant main effects on DL (Y_1), with D/L responsible for the most prominent effects, as evidenced by its high *F*-value (Table III). O/A also displayed significant quadratic effects on DL.

Similarly, O/A (X_1) and D/L (X_2) exhibited significant main effects on EE (Y_2), with O/A also exhibiting significant quadratic effects. O/A (X_1) and Tw20 (X_4) exhibited significant main effects on Rel_{36} (Y_3). O/A (X_1) and Tw20 (X_4) exhibited significant main effects on S_z (Y_4), while O/A and Tw20 also exhibited significant interaction and quadratic effects. Factor coefficient estimates are presented in Table S8.

Response Surface Analysis

The relationships between dependent and independent variables deemed statistically significant were further elucidated using three-dimensional response surface plots. These plots graphically represent the regression equation relating the changes in a response variable against two independent variables at a time, keeping other factors with less significance fixed at their middle levels. Figure 3 depicts the response surface plots, demonstrating the effects of O/A and D/L on DL, effects of O/A and D/L on EE, effects of O/A and Tw20 on Rel_{36}, and effects of O/A and Tw20 on S_z. DL was found to be enhanced, with both an increase in O/A and (to a greater extent) an increase in D/L. EE was elevated by increases in both D/L and, to a greater extent, O/A. Rel_{36} exhibited an increase with increasing Tw20, but a decrease with increasing O/A. Finally, S_z decreased with increasing Tw20, while it initially decreased and then increased with increasing O/A.

Optimization using Desirability Function

The responses Y_1, Y_2, Y_3, and Y_4, were transformed into desirability values d_1, d_2, d_3, and d_4 respectively, while a range was set for factors X_1, X_2, X_3, and X_4. The goals defined for responses Y_1 and Y_2 were maximization, for response Y_3 it was minimization, and for response Y_4 it was a value less than or equal to 150 nm. Equal weight and importance were assigned

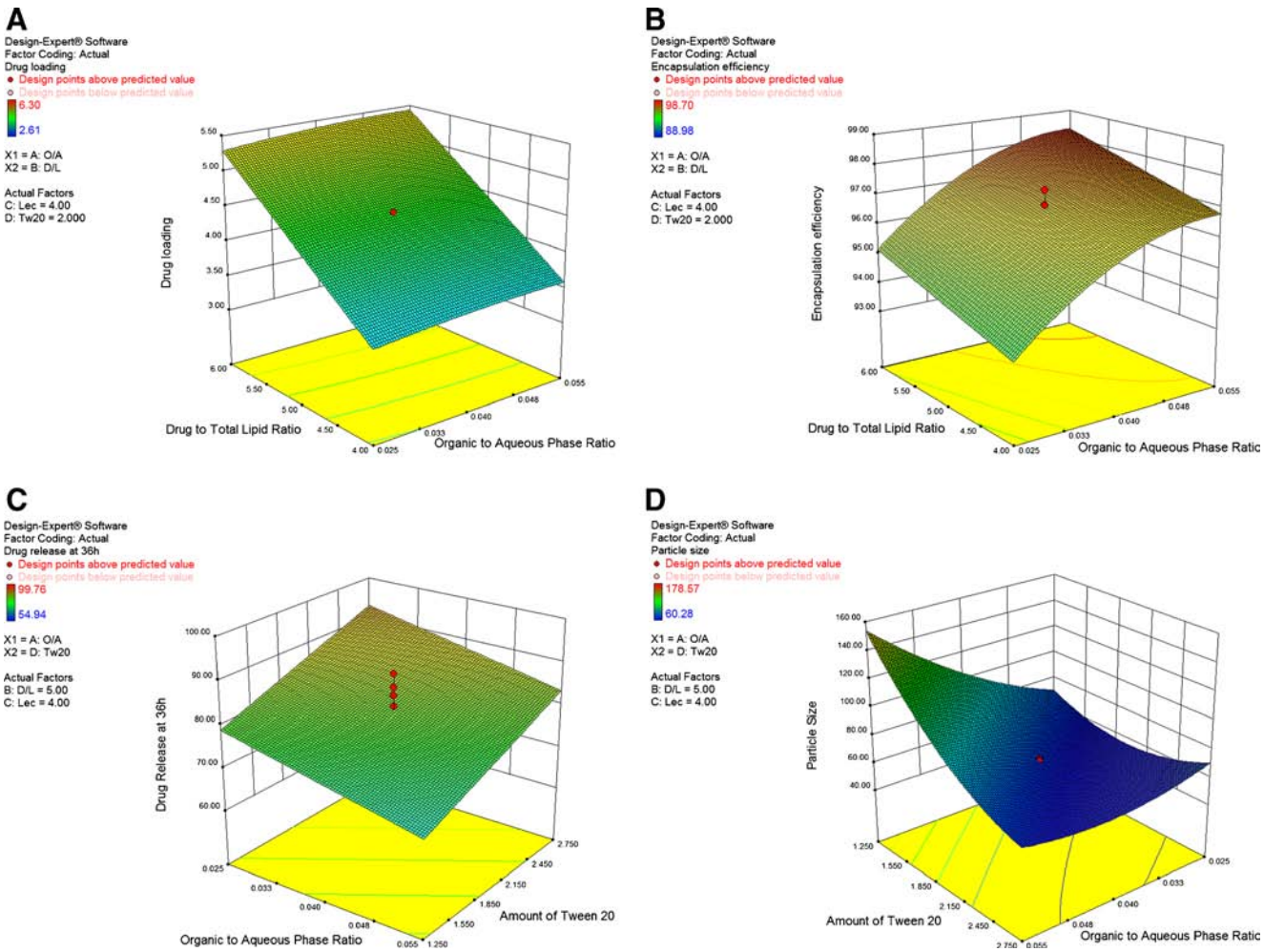

Fig. 3 Central composite design: 3-D response surface plots showing (**a**) effects of drug-to-total lipid ratio and organic-to-aqueous phase ratio on drug loading DL, (**b**) effects of drug-to-total lipid ratio and organic-to-aqueous phase ratio on encapsulation efficiency, (**c**) effects of amount of Tween® 20 and organic-to-aqueous phase ratio on *in vitro* drug release at 36 h, and (**d**) effects of amount of Tween® 20 and organic-to-aqueous phase ratio on particle size.

to each response. The optimal solution (highest desirability) exhibited a desirability of 0.796 and included an O/A of 0.054, D/L of 6%w/w, Lec of 2.5%w/w, and Tw20 of 1.25%w/v. Three optimized formulations at these factor levels were prepared and evaluated to ensure adequate prediction capability of the model (Table IV). All observed values were found to be in good agreement with the predicted values, with no statistical differences detected.

Characterization of IMT-NLC

The optimized IMT-NLC particles exhibited a size of 148.8± 1.4 nm (Fig. 4a), with a PDI of 0.191±0.017. The ζ-potential, which is representative of the surface charge of the nanoparticles, was −23.0±1.5 mV. DL and EE of IMT-NLC are shown in Table IV. TEM images of IMT-NLC (Fig. 4b) indicate that IMT-NLC exists as distinct spherical particles of approximately 140-nm diameter with a dense core, which is consistent with the parameters estimated by DLS.

Solid state characterization of the freeze-dried IMT-NLC was performed by comparing DSC thermograms (Fig. 4c) and XRD patterns (Fig. 4d) of IMT-NLC against those of freeze-dried blank NLC, solid lipid (PcA), and IMT. DSC thermograms of IMT showed a sharp endothermic peak at 211°C to 216°C, which corresponds to the melting point of the drug. No peak was observed in that region for IMT-NLC. Similarly, XRD patterns showed characteristic peaks at 17.2, 18.1, 19.7, 21.1, 24.2 and 25.3° for IMT, which did not appear with IMT-NLC.

Physical Stability

The changes in S_z, PDI and EE of IMT-NLC upon storage at 4°C over a period of 60 days have been recorded in Table V. Over the storage period, S_z appeared to progressively increase very slightly; PDI remained close to 0.200; while EE appeared to progressively decrease very slightly. However, neither S_z nor EE changed significantly over entire 60-days storage period, which implied to incredible physical stability.

Table IV Predicted and Observed Response Values for the Optimized Formulation

Response	Prediction	95% Confidence Interval		Observation[a]
		Low	High	
Drug loading (%w/w)	5.48	5.46	5.51	5.48±0.01[b]
Encapsulation efficiency (%w/w)	98.34	97.90	98.79	97.93±0.03[b]
In vitro drug release at 36 h (%)	69.60	64.81	74.40	65.38±4.22[b]
Particle size (nm)	150.00	145.89	154.11	148.80±1.37[b]

[a] values expressed as mean ± SD ($n=3$)

[b] no significant difference from the predicted response value at $P<0.05$

In vitro Release Kinetics

The *in vitro* drug release profiles for IMT-NLC and free IMT have been illustrated in Fig. 5. The cumulative drug release is expressed as a percentage of total loaded-drug released over time. Complete release for free IMT was achieved in 36 h, while the release from IMT-NLC extended up to almost 168 h, with approximately 65% drug released in first 36 h. The release pattern from IMT-NLC exhibited an initial burst release phase, accounting for approximately 55% of the drug release, which was followed by a sustained release phase.

In vitro Cytotoxicity

The *in vitro* cytotoxic effects of free IMT, blank NLC and IMT-NLC on human bronchial carcinoid cell line NLC-H727 are presented in Fig. 6. Blank NLC (0.001–100 μM) did not exhibit any substantial cytotoxic effects, as demonstrated by the cell viability above 90% observed after 48 h treatment, suggesting that the NLC system is compatible with the cells. Conversely, IMT-NLC elicited dose-dependent cytotoxicity, as evidenced by significant dose-dependent inhibitory effect on cell proliferation at drug concentration ranging from 0.001 μM to 100 μM. Notably, IMT-NLC exhibited significantly better cytotoxic effects ($p<0.05$) on NCI-H727 cells as compared with free IMT after 48 h incubation at higher doses of above 5 μM.

Pharmacokinetics

The plasma concentration–time curves for IMT after IV and oral administration of single dose (IV: 10 mg/kg; oral: 20 mg/kg) of free IMT and IMT-NLC to rats are shown in Fig. 7. At all the time points, plasma levels of the drug were higher for rats administered IMT-NLC than for those administered free IMT in both IV and oral administration groups. The pharmacokinetic parameters have been summarized in Table VI. As compared with free IMT, IMT-NLC exhibited more prolonged circulation of the drug in both cases, as suggested by their significantly lower clearance ($p<0.05$) and significantly higher mean residence time ($p<0.05$). IMT-NLC also appeared to increase the bioavailability of the drug, which is implied by significantly higher $AUC_{0-\infty}$ values ($p<0.05$) after both IV and oral administration, with an almost 2.5-fold increase for both routes of administration. Similarly, C_{max} after oral administration appeared to increase by almost 3 folds ($p<0.05$). IMT-NLC also enhanced the half-life of the drug ($p<0.05$) after IV as well as oral administration.

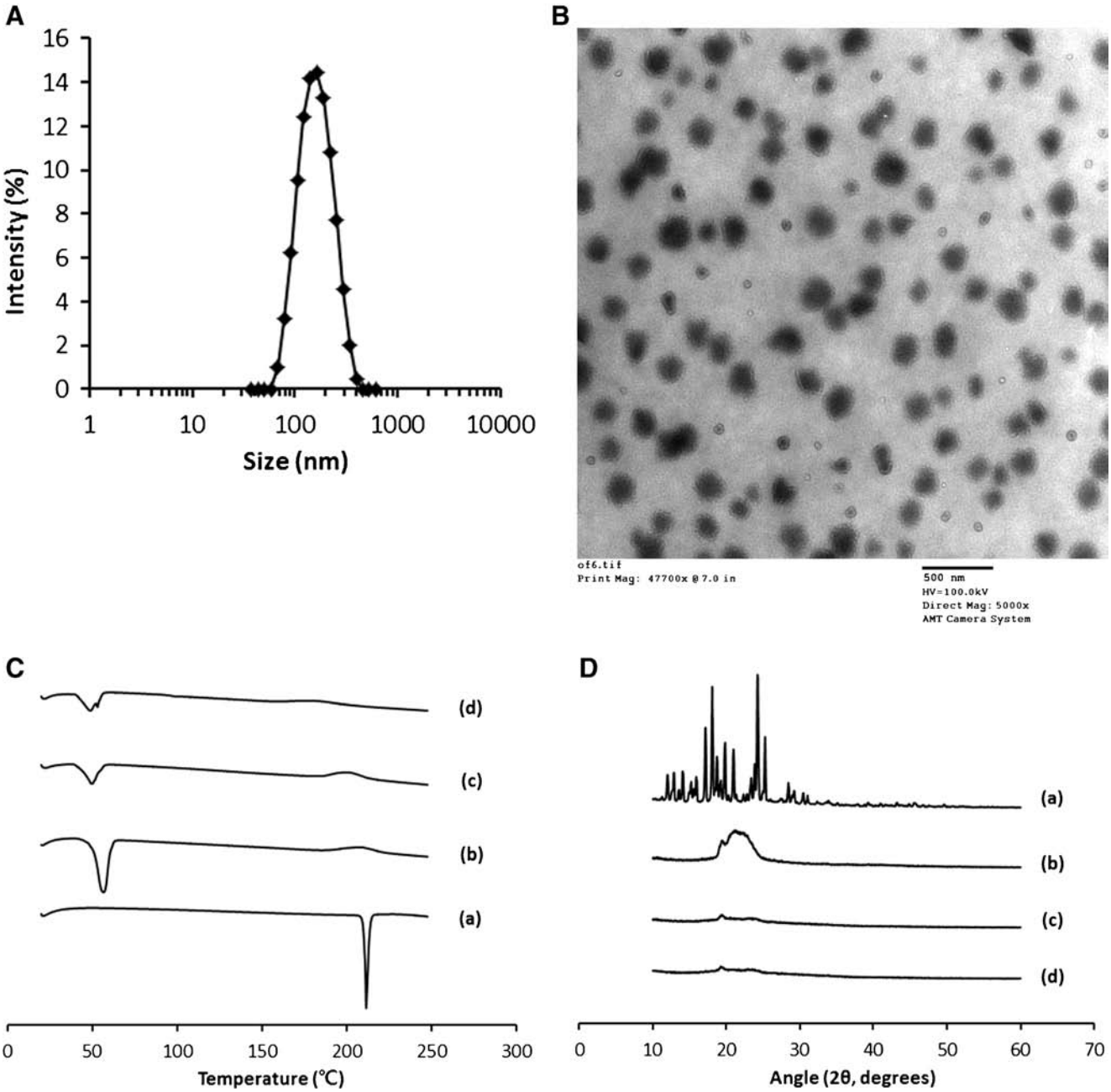

Fig. 4 Characterization of optimized IMT-NLC: (**a**) particle size distribution, (**b**) transmission electron microscopy (TEM) images, (**c**) differential scanning calorimetry (DSC) thermograms, and (**d**) X-ray diffraction (XRD) patterns for (**a**) IMT free base, (**b**) Precirol ATO 5, (**c**) Blank NLC, and (**d**) IMT-NLC.

Table V Effect on Particle Size, PDI and Encapsulation Efficiency upon Storage at 4°C

Day	Particle size (nm)	PDI	EE (%)
1	148.80 ± 1.37	0.191 ± 0.017	97.93 ± 0.03
3	148.87 ± 0.76	0.197 ± 0.017	97.92 ± 0.05
7	149.77 ± 0.93	0.198 ± 0.028	97.89 ± 0.04
15	150.47 ± 2.75	0.194 ± 0.009	97.78 ± 0.08
30	151.50 ± 0.96	0.202 ± 0.013	97.66 ± 0.10
60	153.87 ± 1.03 [a]	0.205 ± 0.004	97.52 ± 0.04**

[a] no significant difference from "Day 1" at $P < 0.05$

DISCUSSION

IMT is a receptor tyrosine kinase inhibitor with specific affinity for Bcr-Abl, PDGFR and c-Kit. It has been shown to be highly effective in the treatment of CML, characterized by over-expression of Bcr-Abl fusion gene, and gastrointestinal stromal tumors (GIST), characterized by over-expression of PDGFR and c-Kit receptors. [20]. The specificity of its anti-proliferative activity provides a strong rationale for use of IMT for targeted cancer therapy. However, clinical applicability of free base form of IMT is limited by its inadequate

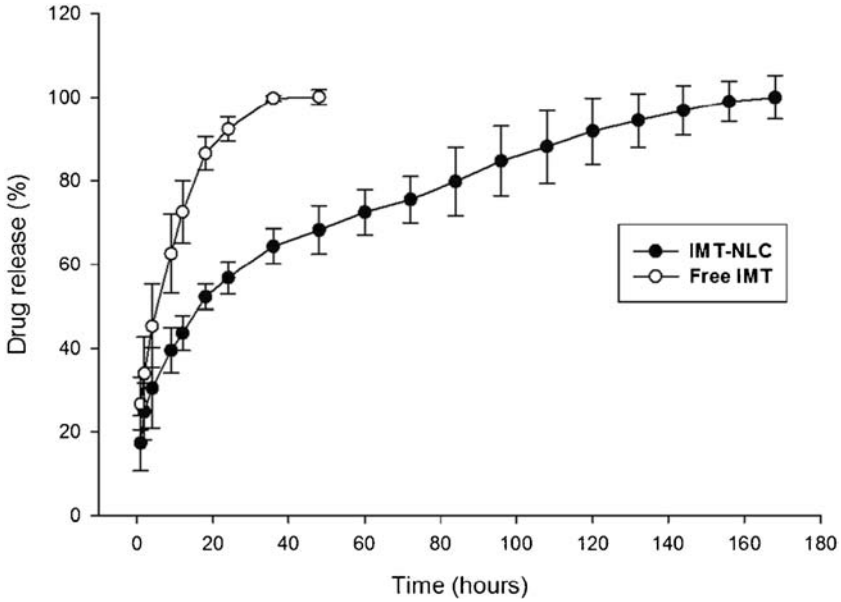

Fig. 5 *In vitro* drug release characteristics of free IMT and IMT-NLC.

pharmacokinetic profile, with low aqueous solubility, extensive first pass metabolism, and rapid clearance [12]. A carrier system allowing encapsulation of the drug with the capability to increase its aqueous solubility and circulation time would greatly enhance its potential anti-cancer applications. NLC is a colloidal carrier capable of enhancing aqueous solubility, permeability and bioavailability of encapsulated drugs [11]. Additionally, long-circulating NLC can be devised utilizing a scheme whereby the carrier system is encased with hydrophilic polymers. The stealth properties thus provided would enable the carrier system to stay in circulation, avoiding clearance by the reticuloendothelial system. Pre-conjugation with lipophilic moieties facilitates more protected attachment of the hydrophilic polymer on the surface of the lipid cores, forming a carrier system with an amphiphilic stealth outer layer [10]. Based on these considerations, IMT-NLC was prepared using TwN and LcN as hydrophilic and hydrophobic surfactants. IMT-NLC preparation factors were optimized using a DoE approach comprising PBD and CCD. This approach not only enabled us to fix optimum levels of all variables for intended performance of IMT-NLC, but also expanded our understanding of the effects of the variables on the critical characteristics of the IMT-NLC system such as particle size, drug encapsulation, and *in vitro* release. Optimized IMT-NLC was characterized and evaluated in terms of *in vitro* release, *in vivo* pharmacokinetics and *in vitro* cytotoxicity.

Response surface methodology (RSM), including CCD and Box-Behnken design, is the most popular and widely

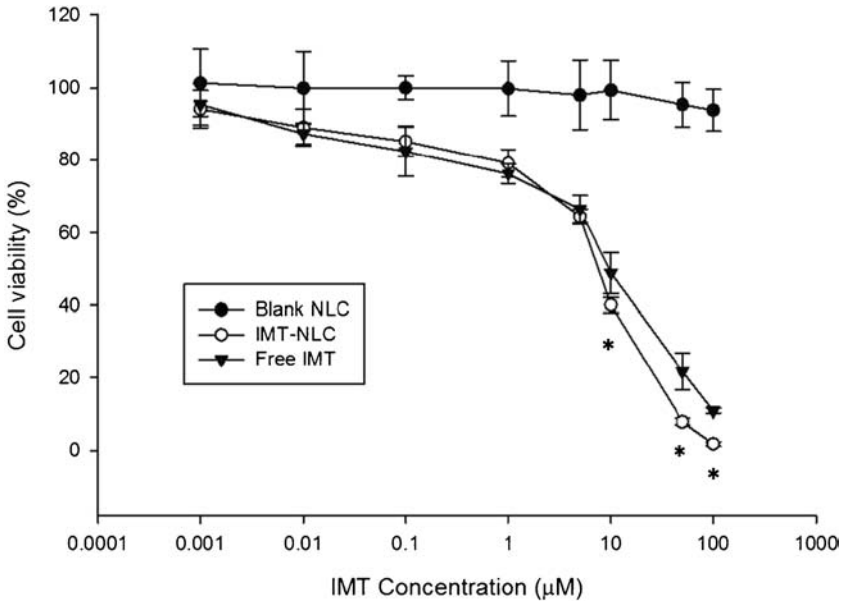

Fig. 6 *In vitro* cytotoxicity characteristics of free IMT and IMT-NLC. * $p < 0.05$ as compared with free IMT. NLC concentrations in blank NLC are the same as those used for the treatment with IMT-NLC.

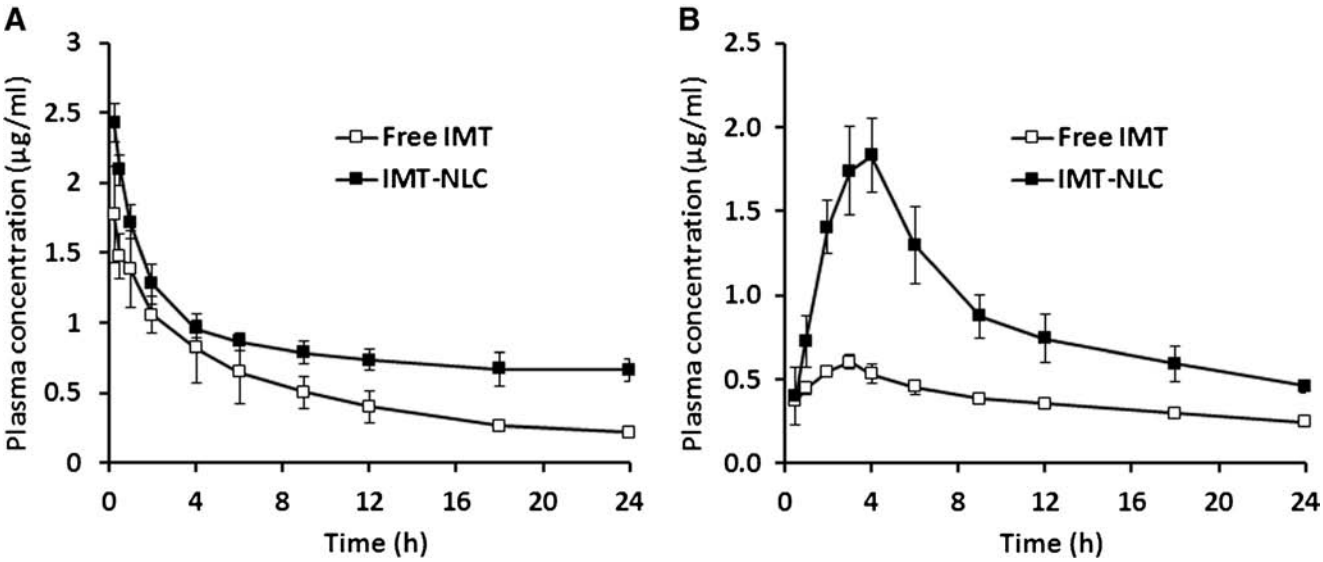

Fig. 7 Plasma concentration–time profiles after intravenous administration (**a**) and oral administration (**b**) of free IMT and IMT-NLC.

recommended approach for the optimization of a process and related parameters, compared with other DoE approaches, especially in situations where interaction effects among the various associated factors cannot be ruled out. While any given process may be associated with numerous factors or variables, identification of the effects of all those variables might be neither possible nor desirable. For this reason, RSM experiments are usually preceded by screening experiments to identify and rule out the insignificant variables using suitable factorial designs such as PBD, Taguchi orthogonal array, and fractional factorial designs [21, 22].

In the present study, eight independent variables were identified that could affect NLC characteristics. An initial screening by PBD was used to identify and exclude the variables that have insignificant main effects on the studied response variables. Consequently, four variables (O/A, D/L, Lec and Tw20) were found to have significant main effects on DL, EE, and S_z of IMT-NLC. A four-factor CCD was, therefore, utilized to optimize the main effects, interaction effects and quadratic effects on DL, EE, Rel_{36}, and S_z of IMT-NLC. D/L, O/A and Lec exhibited significant main effects on DL, with effects of D/L being the most pronounced. DL was enhanced with an increase in D/L and O/A, while it was diminished with an increase in Lec, which was in agreement with previous reports [23]. Increased DL following increase in D/L is associated with the high affinity of the lipid core for the lipophilic drug, which enables accommodation of more of the drug as its concentration increases. Increased DL with increasing O/A can be explained by the fact that higher lipid content makes more lipid matrix available, which is capable of accommodating more of the drug. Decreased DL with increasing Lec likely reflects the strengthening of the nanocarrier stealth with increasing Lec levels, preventing admission of higher amounts of the drug. EE increased with increases in O/A and D/L, conforming to precious reports [24–26]. Increased EE with increasing O/A could be attributed to the fact that increased amount of the lipid

Table VI Pharmacokinetic Parameters of IMT after Administration of IMT and IMT-NLC

Parameters	IV administration (dose: 10 mg/kg)		Oral administration (dose: 20 mg/kg)	
	Free IMT [a]	IMT-NLC [a]	Free IMT [a]	IMT-NLC [a]
C_{max} (µg/ml)	–	–	0.60 ± 0.04	1.79 ± 0.26 [b]
T_{max} (h)	–	–	3.00 ± 0.00	4.00 ± 0.00 [b]
$AUC_{0-\infty}$ (µg*h/ml)	13.77 ± 1.49	34.40 ± 2.45 [b]	17.04 ± 0.54	40.23 ± 2.08 [b]
$T_{1/2}$ (h)	6.71 ± 0.60	14.23 ± 0.95 [b]	22.12 ± 0.96	27.98 ± 2.30 [b]
Ke (h^{-1})	0.104 ± 0.009	0.049 ± 0.003 [b]	0.031 ± 0.001	0.025 ± 0.002 [b]
Cl (ml/h)	228.95 ± 22.95	95.97 ± 6.12 [b]	352.45 ± 11.40	149.42 ± 7.78 [b]
MRT (h)	10.20 ± 0.81	23.74 ± 1.87 [b]	31.47 ± 1.50	36.11 ± 5.09 [b]

C_{max} peak plasma concentration, *T_{max}* time of peak plasma concentration, *$AUC_{0-\infty}$* area under the plasma concentration–time curve, *$T_{1/2}$* plasma half-life, *Ke* elimination rate constant, *Cl* plasma clearance, *MRT* mean residence time

[a] values expressed as mean ± SD ($n = 5$)

[b] significantly different from free IMT at $P < 0.05$

promotes more efficient encapsulation of the lipophilic drug in the lipid matrix. Higher EE with increasing D/L may result from low aqueous solubility and high lipophilicity of the drug [25]. Rel_{36} increased with increasing Tw20, while decreased with increasing O/A, in line with previous reports on the relationship between *in vitro* drug release from lipid and amount of surfactant [27, 28]. The increased drug release with increase in surfactant concentration may be related with the surfactant-induced increase in aqueous solubility of the drug, which would facilitate its diffusion from the lipid matrix to the outer aqueous environment. The observed decrease in drug release from lipid with increased lipid fraction confirms past reports [15] and could be attributed to the enhanced retention of the lipophilic drug by the lipid matrix. Tw20 and O/A exhibited significant main effects on S_z, with S_z decreasing with increasing Tw20, while increasing with increasing O/A, which is in line with previous reports [24, 26]. Reduction in S_z with increase in surfactant concentration may be attributed to reduction in surface tension brought about by increased surfactant concentration, causing reduction in S_z. Conversely, association of increasing S_z with increasing lipid fraction can be accounted for by the increased viscosity of lipid-solvent phase with increasing lipid content, resulting in reduced diffusion rate of the solute molecules to the outer phase and ultimately leading to an increase in S_z [26].

The results of the CCD response surface analysis were used to optimize IMT-NLC by desirability functions approach. The goals for DL and EE were maximization, for Rel_{36} was minimization, and for S_z was less than or equal to 150 nm. While maximization of DL and EE is necessary to ensure delivery of maximum amount of the drug to the tumor site, S_z of the carrier system is critical for passive tumor targeting of the drug, often referred to as enhanced permeability and retention (EPR) effect. Particle sizes preferentially below 200 nm appear to be ideally suited to exploit the EPR effect [29, 30]. During storage, nanocarriers usually increase in size over time [9, 29]. Therefore, a constraint of 150 nm was defined to ensure that S_z remained in optimal range for a prolonged period of time. The purpose of minimizing the drug release was to impart sustained release characteristics to the system. Optimized IMT-NLC characteristics were found to be in good agreement with the predicted responses, and thereby verified that the employed experimental design adequately predicted the behavior of the dependent variables in response to changes in independent variables and helped in accurate optimization of the IMT-NLC system.

DLS and TEM characterization revealed that IMT-NLC comprises of distinct spherical particles having a narrow size distribution. The moderate surface charge (~23 mV) may be associated with improved physical and physiological stability in the blood, as reflected in the observed stability of IMT-NLC during storage at 4°C over 60-days period. High DL and EE proved that the carrier system is capable of entrapping a high drug payload. Solid state characterization by DSC and XRD revealed that the drug was well encapsulated within the carrier system either in molecularly dispersed state or in amorphous state. These observations can be correlated with increased aqueous solubility and bioavailability of the drug.

IMT-NLC exhibited a biphasic release pattern, with an initial burst release followed by a sustained release. Similar patterns of drug release from NLC were previously reported [5, 9, 31]. The biphasic release likely reflects the fact that solid lipid, having a higher melting point than the liquid lipid, crystalizes first, forming a core with very little or no liquid lipid, and the liquid lipid forms tiny pockets mainly near the outer shell. Since liquid lipid solubilizes a greater amount of the drug than solid lipid, initial erosion of the carrier releases a greater amount of the drug, resulting in an initial burst release [9]. It should be emphasized that, compared with IMT solubilized in liquid lipid (LbM) only, the IMT-NLC system prolonged the drug release with approximately 65% of the total loaded-drug being released in the initial 36 h compared to almost 100% release observed from IMT solution. These sustained release characteristics of IMT-NLC could be ascribed to the tendency of NLC to prolong the release of drugs [31]. Drug release occurs through diffusion of the drug from the lipid matrix of NLC and subsequent dissolution into the release medium. Since the lipid matrix exhibits high affinity for lipophilic drugs, diffusion of the drug across the matrix is steadied, ultimately resulting in a sustained release of the drug. Such sustained release is important for modifying the pharmacokinetics of the drug, enhancing tumor targeting, and reducing drug related toxicity [5].

The *in vitro* cytotoxicity study on human bronchial carcinoid NCI-H727 cells revealed dose-dependent cytotoxicity of both IMT and IMT-NLC. However, IMT-NLC exhibited significantly greater cytotoxicity, particularly at higher doses of above 5 μM, after 48 h incubation. The enhanced cytotoxicity of IMT-NLC implies increased intracellular uptake facilitated by the lipophilic nature of the carrier system, and was consistent with previously reported works [6, 32]. Conversely, NLC system without the anti-cancer drug exhibited no significant cytotoxic activity, which is indicative of high compatibility of the drug delivery system with the cells.

Pharmacokinetic parameters of IMT were greatly improved following administration as IMT-NLC by both IV and oral routes, compared to the administration of bulk drug. For both routes of administration, $AUC_{0-\infty}$ was approximately 2.5-fold higher with IMT-NLC, which is indicative of enhanced bioavailability of the drug. $T_{1/2}$ and MRT of the drug were significantly increased, indicating that the drug remains in circulation for a significantly longer period of time. Along with nano-sized architecture of the carrier system, its ability to persist in the blood circulation is necessary for its capability to exploit the EPR effect [30]. Therefore, IMT-NLC ensures increased passive targeting of the drug to the tumor site. The stealth provided by the hydrophilic surfactant layer against clearance by the reticuloendothelial system may be credited for the increased circulation time of

IMT-NLC. In addition to improved $AUC_{0-\infty}$ and $T_{1/2}$, a 3-fold increase in C_{max} was observed after oral administration of IMT-NLC, likely reflecting improved solubility and absorption, which are further indicators of improved bioavailability of the drug.

CONCLUSION

Our study demonstrated that NLC system can be utilized to successfully encapsulate IMT free base, significantly improving the *in vitro* and *in vivo* characteristics of the drug. Optimization by DoE helped to improve our understanding of the factors involved and predict relationships between various independent and dependent variables associated with IMT-NLC system, facilitating the preparation of a formulation capable of optimal performance. In conclusion, the findings of the present work suggest that a combined DoE approach affords accurate optimization of formulation variables, leading to preparation of IMT-NLC exhibiting enhanced *in vitro* and *in vivo* characteristics with tremendous potential for targeted tumor therapy.

ACKNOWLEDGMENTS AND DISCLOSURES

This research was supported by Yeungnam University research grants in 2013.

REFERENCES

1. Muller RH, Radtke M, Wissing SA. Nanostructured lipid matrices for improved microencapsulation of drugs. Int J Pharm. 2002;242:121–8.
2. Joshi MD, Müller RH. Lipid nanoparticles for parenteral delivery of actives. Eur J Pharm Biopharm. 2009;71:161–72.
3. Liu L, Tang Y, Gao C, Li Y, Chen S, Xiong T, *et al.* Characterization and biodistribution *in vivo* of quercetin-loaded cationic nanostructured lipid carriers. Colloids Surf B: Biointerfaces. 2014;115:125–31.
4. Zhang T, Chen J, Zhang Y, Shen Q, Pan W. Characterization and evaluation of nanostructured lipid carrier as a vehicle for oral delivery of etoposide. Eur J Pharm Sci. 2011;43:174–9.
5. Mussi SV, Sawant R, Perche F, Oliveira MC, Azevedo RB, Ferreira LAM, *et al.* Novel nanostructured lipid carrier co-loaded with doxorubicin and docosahexaenoic acid demonstrates enhanced in vitro activity and overcomes drug resistance in MCF-7/Adr cells [published online ahead of print Feb 13 20014]. Pharm Res. 2014. doi:10.1007/s11095-013-1290-2.
6. Liu D, Liu Z, Wang L, Zhang C, Zhang N. Nanostructured lipid carriers as novel carrier for parenteral delivery of docetaxel. Colloids Surf B: Biointerfaces. 2011;85:262–9.
7. Zhang XG, Miao J, Dai YQ, Du YZ, Yuan H, Hu FQ. Reversal activity of nanostructured lipid carriers loading cytotoxic drug in multi-drug resistant cancer cells. Int J Pharm. 2008;361:239–44.
8. Taratula O, Kuzmov A, Shah M, Garbuzenko OB, Minko T. Nanostructured lipid carriers as multifunctional nanomedicine platform for pulmonary co-delivery of anticancer drugs and siRNA. J Control Rel. 2013;171:349–57.
9. Zhang XY, Qiao H, Ni JM, Shi YB, Qiang Y. Preparation of isoliquiritigenin-loaded nanostructured lipid carrier and the *in vivo* evaluation in tumor-bearing mice. Eur J Pharm Sci. 2013;49:411–22.
10. Selvamuthukumar S, Velmurugan R. Nanostructured lipid carriers: a potential drug carrier for cancer chemotherapy. Lipids Health Dis. 2012;11:159. Available from: http://www.lipidworld.com/content/11/1/159.
11. Fang CL, Al-Suwayeh SA, Fang JY. Nanostructured lipid carriers (NLCs) for drug delivery and targeting. Recent Pat Nanotechnol. 2013;7:41–55.
12. Al-Hadiya BMH, Bakheit AHH, Abd-Elgalil AA. Imatinib mesylate. In: Brittain HG, editor. Profiles of drug substances, excipients, and related methodology, Volume 39. Elsevier Inc. p. 265–297. Available from: http://dx.doi.org/10.1016/B978-0-12-800173-8.00006-4
13. Gündüz H, Özlü Y, Yal in S. Process for the preparation of imatinib base. US Patent No. US 8,252,926 B2. 2012 Aug 28.
14. Lionberger RA, Lee SL, Lee LM, Raw A, Yu LX. Quality by design: concepts for ANDAs. AAPS J. 2008;10(2):268–76.
15. Poudel BK, Marasini N, Tran TH, Choi HG, Yong CS, Kim JO. Formulation, characterization and optimization of valsartan self-microemulsifying drug delivery system using statistical design of experiment. Chem Pharm Bull. 2012;60(11):1409–18.
16. Dejaegher B, Heyden YV. Experimental designs and their recent advances in set-up, data interpretation, and analytical applications. J Pharm Biomed Anal. 2011;56:141–58.
17. Velpandian T, Mathur R, Agarwal NK, Arora B, Kumar L, Gupta SK. Development and validation of a simple liquid chromatographic method with ultraviolet detection for the determination of imatinib in biological samples. J Chromatogr B. 2004;804:431–4.
18. Müller RH, Mäder K, Gohla S. Solid lipid nanoparticles (SLN) for controlled drug delivery – a review of the state of the art. Eur J Pharm Biopharm. 2000;50:161–77.
19. Derringer G, Suich R. Simultaneous optimization of several response variables. J Qual Tech. 1980;12(4):214–9.
20. Deininger M, Buchdunger E, Druker BJ. The development of imatinib as a therapeutic agent for chronic myeloid leukemia. Blood. 2005;105(7):2640–53.
21. Baş D, Boyacı İH. Modeling and optimization I: usability of response surface methodology. J Food Eng. 2007;78:836–345.
22. Bezerra MA, Santelli RE, Oliveira EP, Villar LS, Escaleira LA. Response surface methodology (RSM) as a tool for optimization in analytical chemistry. Talanta. 2008;76:965–77.
23. Zhang X, Liu J, Qiao H, Liu H, Ni J, Zhang W, *et al.* Formulation optimization of dihydroartemisinin nanostructured lipid carrier using response surface methodology. Powder Technol. 2010;197:120–8.
24. Kudarha R, Dhas NL, Pandey A, Belgamwar VS, Ige PP. Box-Behnken study design for optimization of bicalutamide-loaded nanostructured lipid carrier: stability assessment [published online ahead of print May 2, 2014]. Pharm Dev Technol. 2014. doi:10.3109/10837450.2014.908305.
25. Liu CH, Wu CT. Optimization of nanostructured lipid carriers for lutein delivery. Colloids Surf A Physicochem Eng Asp. 2010;353:149–56.
26. Keshri L, Pathak K. Development of thermodynamically stable nanostructured lipid carrier system using central composite design for zero order permeation of econazole nitrate through epidermis. Pharm Dev Technol. 2013;18(3):634–44.
27. Kalam MA, Sultana Y, Ali A, Aqil M, Mishra AK, Aljuffali IA, *et al.* Part I: development and optimization of solid-lipid nanoparticles using Box-Behnken statistical design for ocular delivery of gatifloxacin. J Biomed Mater Res Part A. 2013;101A:1813–27.
28. Marasini N, Yan YD, Poudel BK, Choi HG, Yong CS, Kim JO. Development and optimization of self-nanoemulsifying drug delivery system with enhanced bioavailability by Box-Behnken design and desirability function. J Pharm Sci. 2012;101(12):4584–96.

29. Tran TH, Ramasamy T, Truong DH, Shin BS, Choi HG, Yong CS, *et al.* Development of vorinostat-loaded solid lipid nanoparticles to enhance pharmacokinetics and efficacy against multidrug-resistant cancer cells [published online ahead of print Feb 22, 2014]. Pharm Res. 2014. doi:10.1007/s11095-014-1300-z.
30. Sofou S. Radionuclide carriers for targeting of cancer. Int J Nanomed. 2008;3(2):181–99.
31. Yang X, Li Y, Li M, Zhang L, Feng L, Zhang N. Hyaluronic acid-coated nanostructured lipid carriers for targeting paclitaxel to cancer. Cancer Lett. 2013;334:338–45.
32. Bondì ML, Craparo EF, Giammona G, Cervello M, Azzolina A, Diana P, *et al.* Nanostructured lipid carriers-containing anticancer compounds: preparation, characterization, and cytotoxicity studies. Drug Deliv. 2007;14:61–7.